Robust Dynamic Sliding Mode Control of a Deployable Cable Driven Robot

S. A. Khalilpour*, R. Khorrambakht *, M. J. Harandi*, H. D. Taghirad * and Philippe Cardou †

*Advanced Robotics and Automated Systems (ARAS), Faculty of Electrical Engineering
K. N. Toosi University of Technology, P.O. Box 16315-1355, Tehran, Iran.
Email: khalilpour@ee.kntu.ac.ir, r.khorrambakht, jafari@email.kntu.ac.ir taghirad@kntu.ac.ir

† Department of Mechanical Engineering, Robotics Laboratory, Laval University,
Quebec City, QC G1V 0A6, Canada, Email: pcardou@gmc.ulaval.ca

***Abstract*—Despite of bing intensively developed, cable driven parallel manipulators are not yet vastly used due to their requirements for accurate assembly and installation. The main goal of this paper is to propose a suitable control method by which the robot could be suitably controlled without the requirement for undergoing any accurate calibration process. Here this robot is called deployable cable driven manipulator, in which the positions of the cable attachment points are not accurately known. This uncertainty in measurements will affect many parameters in the kinematic model especially the Jacobian matrix which is used as a force distributer in the Cartesian-space control strategies. In this paper in order to overcome this problem, a robust dynamic sliding mode controller is proposed. Then robust stability of the closed-loop system is analyzed through the Lyapunov direct method and by accordingly appropriate controller gain selection is performed. In order to illustrate the performance of the proposed controller, the robot is simulated in ADAMS software and it is shown that a suitable controller performance could be achieved.**

***Index Terms*—Uncertain Jaconian, Cable Driven Parallel Manipulator, Robust control, Dynamic sliding mode control.**

I. Introduction

In a Cable Driven Parallel Manipulator (CDPM), the end effector is linked to the actuators installed on the fixed frame using several flexible cables. Large work space, great speed and high acceleration alongside with the simple mechanical structure are among the advantages of this robots. The idea of cable robots being easily and rapidly deployed was first proposed in [1], [2], [3] to be utilized in help and rescue missions. In fact, large workspace, capability of carrying heavy loads and possibility of rapid installation make this classes of robots suitable in many rescue missions [4]. Agriculture and automated farm lands are also potential applications in which the concept of deployable cable driven robots could be utilized.[1].

In Deployable Suspended Cable-driven Robots (DSCRs), the kinematic parameters are not accurately measured, and as a result, characteristics of the robot's model is perturbed. This in turn introduces many challenges in terms of controller design and meeting the required performance [2], [5], [6], [7], [8], [9].

Fig. 1. Prototype of a deployable suspended cable driven robot called ARAS-CAM.

Nowadays, a family of cable driven robots known as Spidercams are commonly used for video capturing of sport games. As shown in the Figure 1, ARAS-CAM robot is an example of a Deployable Suspended Cable driven Robot (DSCR) which is specially designed for imaging purposes. The simplicity of installation as the main characteristic of DSCR makes it extremely suitable for the field of imaging.

There is several successful robust controllers applied to various applications in the literature. As an example, sliding mode controllers are well-known for their effectiveness in

978-1-5386-4916-9/18/$31.00

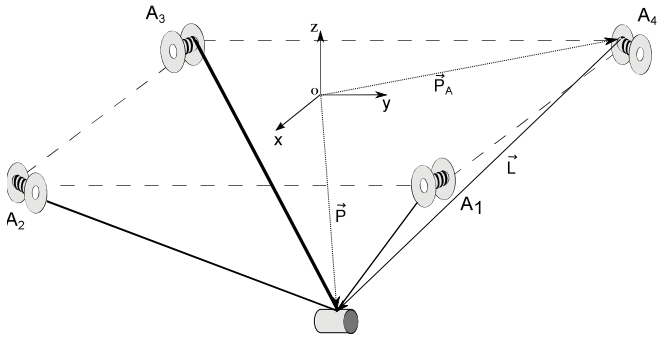

Fig. 2. Kinematic schematics of deployable suspended cable robot.

many problems [10], [11]. Therefore, in this work a robust sliding mode controller is proposed in order to account for the kinematic uncertainties. As reported in many references [12], [11], despite of proper designed controllers, undesired oscillations could still manifest in the system outputs. This phenomenon, called chattering, is generally caused by discrete implementation, unmodeled actuator dynamics and presence of disturbances [13], [14].

The main goal of this work has been to develop a dynamic sliding mode robust controller by which The DSCR could be suitably controlled without any requirements for accurate calibration processes. In dynamic sliding control method, a new switching function[15], [16], [17] composed of the first or higher order derivatives of the control input is utilized [18], [19] and the discontinuities in control inputs are shifted to the first or high order derivatives. As a result a continuous dynamic sliding mode control law could be obtained in which the chatting phenomenon is significantly reduced [19].

The remaining of this paper is constructed as follows: first the kinematic model of a DSCR is studied and the Jacobian matrix is derived. In the next section, the proposed robust control law is introduced and then robust stability of the closed loop system is analyzed. Finally in the last section, the ability of the proposed controller to achieve suitable performance is illustrated through simulation.

II. Kinematic Modeling

This section is devoted to deriving the kinematic model of DSCR. To this end, first the inverse kinematics of the robot is derived then by differentiation, the Jacobian matrix is formulated. Fig. 2 illustrates a DSCR with four cables. As shown in Fig.2, all cables are attached to a single point on the end-effector and using the tension in the cables, the end-effector could be controlled. Typically, the end-effector is modeled as a lumped mass located at the point of cable intersections. The loop closure for this manipulator is formulated as shown in Fig. 2 is given as follows.

$$\overrightarrow{L_i} = \overrightarrow{P} - \overrightarrow{P_{A_i}}, \quad i = 1,\ldots,4. \tag{1}$$

In what follows, inverse kinematics relations and the Jacobian matrix are derived.

A. Inverse Kinematics Solution

Algebraically rewriting the loop closure equation gives:

$$(l_i)^2 = (P - P_{A_i})^T (P - P_{A_i}) \tag{2}$$

where l_i is the length of i'th cable. Rewriting this equation componentwise leads to:

$$l_i = \sqrt{(x-x_i)^2 + (y-y_i)^2 + (z-z_i)^2} \tag{3}$$

in which, the x, y, z and x_i, y_i, z_i, respectively denote the position of end-effector and attachment points of the i'th cable.

B. Jacobian Matrix

The Jacobian matrix plays an important role in the kinematics problem analysis due to the fact that it reveals important relationships between the work and joint space. In other words, Jacobian matrix performs a mapping between the joint and task space variables. The jacobian matrix constructs a transformation which maps the actuator forces to the forces and moments acting on the moving platform [20]. Furthermore, an important kinematic problem, the singularity analyses, can be studied through the Jacobian matrix. So considering the it's importance, in what follows, the Jacobian matrix of DCSR is derived.

Letting l denote the vector of joint coordinates containing the lengths of the cables and x, the vector of end-effector motion variables, the kinematics equations can be derived as $f(l,x) = 0$, an implicit function of vectors x and l. Through derivative of $f(l,x)$, the relation between the joint space and work space velocities $\dot{l}$, $\dot{x}$ is achieved:

$$J_x \dot{x} = J_l \dot{l} \tag{4}$$

$$J_x = +\frac{\partial f}{\partial x}, \qquad J_l = -\frac{\partial f}{\partial l} \tag{5}$$

So the jacobian matrix can be derived as follows:

$$\dot{l} = J\dot{x} \tag{6}$$

$$J = J_L^{-1} J_x \tag{7}$$

Finally, The analytical form of Jacobian matrix of the robot shown in Fig. 2 is as follows:

$$J = \begin{bmatrix} \frac{(x-x_1)}{l1} & \frac{(y-y_1)}{l1} & \frac{(z-z_1)}{l1} \\ \frac{(x-x_2)}{l2} & \frac{(y-y_2)}{l2} & \frac{(z-z_2)}{l2} \\ \frac{(x-x_3)}{l3} & \frac{(y-y_3)}{l3} & \frac{(z-z_3)}{l3} \\ \frac{(x-x_4)}{l4} & \frac{(y-y_4)}{l4} & \frac{(z-z_4)}{l4} \end{bmatrix} \tag{8}$$

III. Dynamic Sliding Mode

Neglecting the flexibility of the cables, the dynamic model of DSCR may be written as:

$$M(x)\ddot{x} + C(x,\dot{x})\dot{x} + G = F = -J\boldsymbol{\tau} \tag{9}$$

in which M, C and G denote respectively mass matrix, Coriolis term and gravity vector. Also x and F are vectors respectively denoting the generalized coordinates of the end-effector position and the Cartesian wrench applied to it. also

J denotes the Jacobian matrix of the robot and $\boldsymbol{\tau}$ the vector of cable forces.

Some important properties of the derived dynamics equation are as follows:

property 1: The matrix $M(x)$ is symmetric and positive definite and upper and lower bounded for all x [14]

$$\lambda_m < ||M(x)|| < \lambda_M \tag{10}$$

where λ_m and λ_M denote the minimum and maximum eigenvalues of the matrix M, respectively.

property 2: The $C(X,\dot{X})$ matrix and the time derivative of inertia matrix $M(X)$ satisfy

$$\dot{x}^T \left[\frac{1}{2}\dot{M}(x) - C(x,\dot{x})\right]\dot{x} = 0 \tag{11}$$

which shows that the matrix $\dot{M}(x) - 2C(x,\dot{x})$ is skew-symmetric.

property 3: The upper bounds of Coriolis and centrifugal matrices are functions of $\dot{x}$:

$$||C(x,\dot{x})|| < \zeta_c||\dot{x}|| \tag{12}$$

property 4: The upper bound of gravity matrix is limited:

$$||G(x)|| < \zeta_g \tag{13}$$

The cartesian error manifold is defined as:

$$s_r = \dot{x} - \dot{x}_r \tag{14}$$

where x_r is defined as a Cartesian nominal reference for motion control and is designed as

$$\dot{x}_r = \dot{x}_d - \boldsymbol{\Lambda}\tilde{x} + s_d - \gamma\sigma \tag{15}$$

$$\dot{\sigma} = \mathrm{sgn}(s_x) \tag{16}$$

in which $\dot{x}_d$ is the desired velocity of the end-effector and $\tilde{x} = x - x_d, \gamma \in R^{n\times n}$. The function sgn(.) stands for the inputwise discontinuous signum function. Also $\boldsymbol{\Lambda} = diag(\Lambda_1, \Lambda_2, \cdots, \Lambda_n)$ is a symmetric positive definite diagonal matrix and n denotes the degrees of freedom of the robot. A sliding surface vector is defined as follows:

$$s = \dot{\tilde{x}} + \boldsymbol{\Lambda}\tilde{x} \tag{17}$$

and

$$s_x = s - s_d \tag{18}$$

$$s_d = s(t_0)e^{-k(t-t_0)} \tag{19}$$

in which k is a positive number and $s(t_0)$ is the value of $s(t)$ at the time t_0. Thus, $s_x(t_0) = 0$ and $s_x(t)$ are exponentially converged to $s(t)$. It can be shown that the relation between s_x and s_r is derived as follows:

$$s_r = s_x + \gamma\sigma \tag{20}$$

The equation 9 can be written in terms of a nominal reference $\dot{x}_r$, and its derivative $\ddot{x}_r$, as follows:

$$M\ddot{x}_r + C\dot{x}_r + G = Y\boldsymbol{\theta} \tag{21}$$

as proved in [15], [16], [17], the equation 21 bounded, $Y\boldsymbol{\theta} < \eta(t)$, because the nominal reference $\dot{x}_r$, and its derivative are also bounded as $||\dot{x}_r|| < \beta_1 + \beta_2||\tilde{x}|| + \gamma\sigma$ and $||\ddot{x}_r|| < \beta_3 + \beta_4||\tilde{\dot{x}}||$, respectively.

A. The proposed control law

Let the control law to be defined as follows:

$$F = -K_d s_r + \hat{M}\ddot{x}_r + \hat{C}\dot{x}_r + \hat{G} \tag{22}$$

where K_d is a symmetric diagonal positive definite matrix and $\hat{J}$ is the roughly approximate Jacobian matrix. For the fully actuated robots, the actuator forces are calculated as $\boldsymbol{\tau} = -\hat{J}^{\dagger}F$, But due to the redundancy in redundant robots like ARAS-CAM, the jacobian is not a square matrix. Therefore, the actuator forces, $\boldsymbol{\tau}$, should be obtained by solving a redundancy resolution problem. Also, $\hat{M}$, $\hat{C}$ and $\hat{G}$ respectively denote the approximate mass matrix, coriolis term and gravity vector. Furthermore, the tension in the cables are:

$$\boldsymbol{\tau} = \bar{\boldsymbol{\tau}} + \alpha Q \tag{23}$$

where

$$\bar{\boldsymbol{\tau}} = -\hat{J}^{\dagger}F \tag{24}$$

where $\hat{J}^{\dagger} = \hat{J}(\hat{J}^T\hat{J})^{-1}$ and Q is the null space of the approximated jacobian. Also, α is a scalar factor which is selected so that actuator forces remain in the feasible range $[\tau_{\min}, \tau_{\max}]$.

B. Stability Analysis

To analyze the stability of the proposed control laws, consider the following Lyapunov function candidate

$$V(t) = \frac{1}{2}s_r^T M s_r \tag{25}$$

differentiating $V(t)$ with respect to time gives:

$$\dot{V}(t) = s_r M\dot{s}_r + s_r C s_r \tag{26}$$

According to 14, it can be written:

$$\dot{s}_r = \ddot{x} - \ddot{x}_r \tag{27}$$

By substituting 27 in 9

$$M\dot{s}_r = -Cs_r - (M\ddot{x}_r + C\dot{x}_r + G) - J^T\tau \tag{28}$$

using 28, 26 becomes

$$\dot{V}(t) = s_r(M\ddot{x}_r + C\dot{x}_r + G - J^T\tau) \tag{29}$$

substituting $\boldsymbol{\tau} = -\hat{J}^{\dagger}F + Q$ in equation 31

$$\begin{aligned}\dot{V} &= s_r(-(M\ddot{x}_r + C\dot{x}_r + G) - J^T(-\hat{J}^{\dagger}F + Q)) \\ &= s_r(-(M\ddot{x}_r + C\dot{x}_r + G) + J^T\hat{J}^{\dagger}F - Q + F - F + \hat{J}^T Q) \\ &= s_r(-(M\ddot{x}_r + C\dot{x}_r + G) - (I - J^T\hat{J}^{\dagger})F - (J^T - \hat{J}^T)Q + F)\end{aligned} \tag{30}$$

considering $F = -Ks_r + \hat{M}\ddot{x}_r + \hat{C}\dot{x}_r + \hat{G}$, we have:

$$\dot{V} = s_r((\tilde{M}\ddot{x}_r + \tilde{C}\dot{x}_r + \tilde{G}) - (I - J^T\hat{J}^{\dagger})F - (J^T - \hat{J}^T)Q - Ks_r) \tag{31}$$

where

$$\tilde{M} = \hat{M} - M, \qquad \tilde{C} = \hat{C} - C, \qquad \tilde{G} = \hat{G} - G \tag{32}$$

Based on uncertain Jacobian matrix J^T , and the internal forces being bounded, the following equation may be assumed to be bounded:

$$||(I - J^T \hat{J}^{\dagger})F|| < \zeta_J s_r \tag{33}$$

$$||(J^T - \hat{J}^T)Q|| < \zeta_Q \tag{34}$$

Taking the equations 33 and 34 into account, the equation 31 can be rewritten in an inequality form as:

$$\dot{v} < -K||s_r||^2 - \zeta_J||s_r||^2 - (\tilde{\eta} + \zeta_Q)||s_r|| \tag{35}$$

where $\tilde{\eta}$ is the upper bound of $Y\hat{\Theta} - Y\Theta = \tilde{M}\ddot{x}_r + \tilde{C}\dot{x}_r + \tilde{G}$.

Therefore, selecting a large enough value for k and assuming $s_r(t_0) < \varepsilon$, the tracking error is upper bounded and converges to ε.

Now we prove that the sliding surface s_x also converges to a bounded limit. To this end, first it is shown that the $\dot{s}_r$ is bounded.

$$\begin{aligned}
\dot{s}_r =& M^{-1}(-Cs_r - (M\ddot{x}_r + C\dot{x}_r + G) + \cdots \\
& - J^T(-\hat{J}^{\dagger}F + Q + F - F + \hat{J}Q) \\
=& -M^{-1}(Cs_r + (\tilde{M}\ddot{x}_r + \tilde{C}\dot{x}_r + \tilde{G}) + (I - J^T\hat{J}^{\dagger})F + \cdots \\
& + (J^T - \hat{J})Q - Ks_r) \\
<& \lambda_M(M^{-1})((\lambda_M(K) + \zeta_c||\dot{x}|| + \zeta_J)\varepsilon + \zeta_Q + \tilde{\eta}) \\
<& \zeta_{\dot{s}_r}(t)
\end{aligned} \tag{36}$$

Thus, $\dot{s}_r$ is upper bounded as $\dot{s}_r < \zeta_{\dot{s}_r}(t)$. Now consider the following Lyapanov candidate V_x as

$$V_x = \frac{1}{2} s_x^T s_x \tag{37}$$

Differentiating V_x with respect to time and substituting $\dot{s_x}$ from differentiation of equation 20 yields:

$$\begin{aligned}
\dot{V}_x =& s_x^T \gamma sgn(s_x) + s_x^T \dot{s}_r \\
& < -\gamma||s_x|| + ||s_x||||\dot{s}_r|| \\
& < -\gamma||s_x|| + \bar{\zeta}||s_x|| \\
& < (\bar{\zeta} - \gamma)||s_x||
\end{aligned} \tag{38}$$

where $\bar{\zeta}$ denotes the supremum of ζ. Thus, in order to prove that s_x converges in a finite time, we can choose

$$\gamma > \bar{\zeta} \tag{39}$$

IV. Simulations

This section is devoted to the simulation of the proposed control method. To this end, first the characteristics of the dynamics modeling implemented in the ADAMS is introduced. Then the performance of the presented algorithm is illustrated.

A. Model Characteristics

In order to model the DSCR in ADAMS software, cables and pulleys structures are used from the machinery toolbox. The considered physical parameters for the cables and pulleys are shown in table I. Also, according to Fig. 2 geometrical parameters of the robot are selected as $a = 3^m$, $b = 4^m$ and $h = 3$. These physical parameters describe the real world ARAS-CAM robot features.

B. Results

In order to verify the effectiveness of the proposed controller, the simulations are performed and the results of the proposed robust dynamic sliding mode controller are shown. It should be noted that the considered uncertainty in the attachment points positions and the mass of the end-effector is 10 percent. Also the gains of the controller are chosen in such a way that the stability of the system in the presence of model uncertainty is granted. So $k_d = [100, 100, 100]$, $\gamma = [0.1, 0.1, 0.5]$ and $\alpha = [50, 50, 50]$ are chosen.

As shown in Fig. 3, the desired trajectory of the end-effector is generated using a cubic trajectory generation algorithm. Figure 3 indicates that the robot has accurately followed the desired trajectory. Also, Figure 4 illustrates the tracking error and figures 5 and 6 depict the variation of manifolds s_r and s_x.

Fig. 7 shows how σ carries out a dynamic displacement of the solution manifold $s_x = 0$, which, in turn, induces a sliding mode at $s_x = 0$.

Figure 8 shows the tensions in the cables during the maneuver of the end-effector. As depicted in Figure 8 all of the forces are positive so all the cables are in tension. Therefore the designed trajectory is in the feasible wrench workspace.

Figure 9 depicts the variations of cables lengths within the robot trajectory. As seen in the figure 9, there is a minimum of one meter variation, in the length of two cables.

V. Conclusions

In this paper, an easy deployable cable driven parallel robot is introduced. Due to its easy installation process the cost of utilization is decreased and transporting it from a place to another introduces no considerable effort. However, the lack of absolute accuracy in installation process would lead to a no perfect operation for the robot. The kinematics uncertainty will influence the performance and degrade the level of achievable

TABLE I
The kinematic and dynamic parameters of the ARAS-CAM.

Parameter	Symbol	value
end effector mass	kg	30
cable density	kg	10^{-6}
Young's modulus of cable	$\frac{N}{m^2}$	10^{11}
pulley friction Coefficient μ	-	0.6
pulley stiffness	$\frac{N}{m^2}$	10^7
Preload	N	0

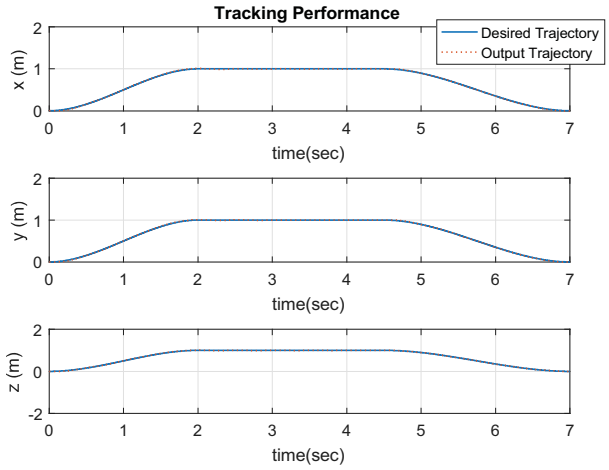

Fig. 3. Performance of Tracking a desired trajectory.

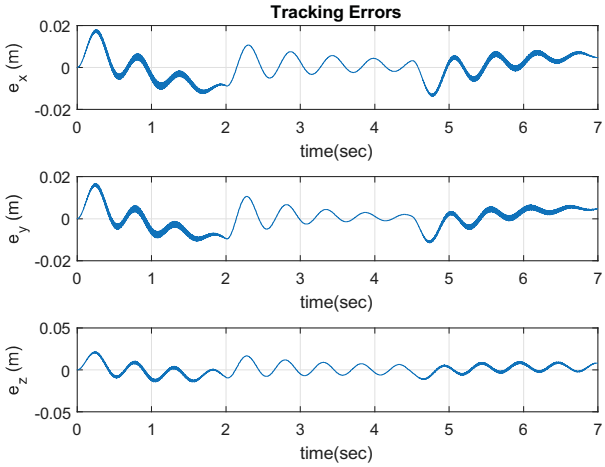

Fig. 4. Tracking error of a desired trajectory.

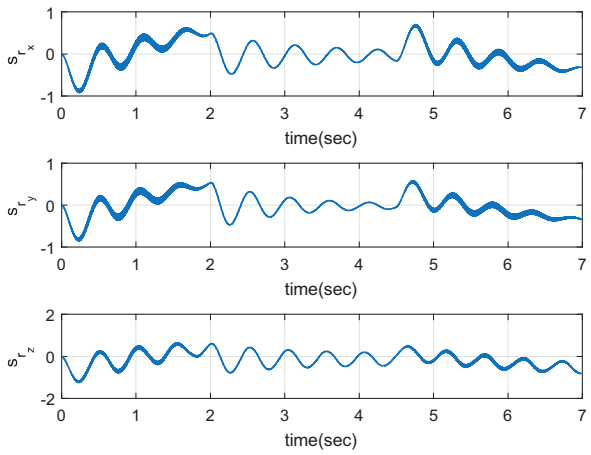

Fig. 5. Cartesian error manifold, s_r.

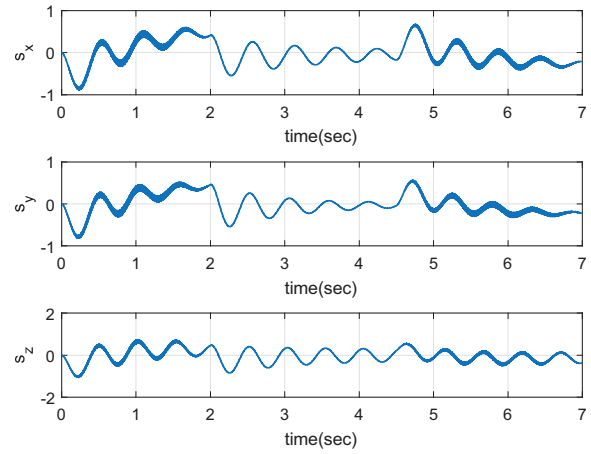

Fig. 6. Sliding vector surface, s_x.

accuracy. So in this paper a robust dynamic sliding mode controller is proposed to control the robot in the presence of such uncertainties. The proposed controller is designed in Cartesian coordinates, as a result, utilization of the inverse kinematics is not required in order to synthesis the trajectory for executing a given task. In addition, the controller keeps all cables in tension for the whole wrench feasible workspace. Finally, the suitable tracking performance of the proposed controller is verified through some simulations.

ACKNOWLEDGMENT

The authors would like to thank Iranian National Science Foundation (INSF) for partially supporting this research work under the grant number **96001803**. Authors greatly appreciate Mr. Salman Kariminasab and Mr. Alireza Bourbour for their contribution in the discussions during this research period.

REFERENCES

[1] B. L. Jordan, M. A. Batalin, and W. J. Kaiser, "Nims rd: A rapidly deployable cable based robot," in *Proceedings 2007 IEEE International Conference on Robotics and Automation*. IEEE, 2007, pp. 144–150.

[2] P. H. Borgstrom, B. L. Jordan, B. J. Borgstrom, M. J. Stealey, G. S. Sukhatme, M. A. Batalin, and W. J. Kaiser, "Nims-pl: a cable-driven robot with self-calibration capabilities," *IEEE Transactions on Robotics*, vol. 25, no. 5, pp. 1005–1015, 2009.

[3] P. Bosscher, R. L. Williams, and M. Tummino, "A concept for rapidly-deployable cable robot search and rescue systems," in *ASME 2005 International Design Engineering Technical Conferences and Computers and Information in Engineering Conference*. American Society of Mechanical Engineers, 2005, pp. 589–598.

[4] J. Merlet, "Marionet, a family of modular wire-driven parallel robots," *Advances in Robot Kinematics: Motion in Man and Machine*, pp. 53–61, 2010.

[5] C. C. Cheah, S. Kawamura, and S. Arimoto, "Feedback control for robotic manipulator with an uncertain jacobian matrix," *Journal of Robotic Systems*, vol. 16, no. 2, pp. 119–134, 1999.

[6] C. C. Cheah, S. Kawamura, S. Arimoto, and K. Lee, "H tuning for task-space feedback control of robot with uncertain jacobian matrix,"

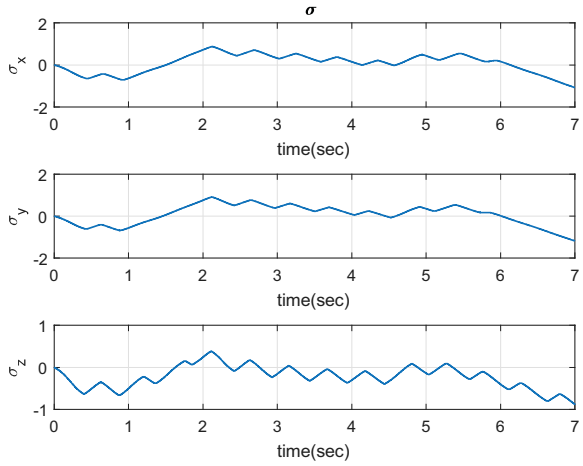

Fig. 7. Variations of $\sigma = \int \mathrm{sgn}(s_x)$

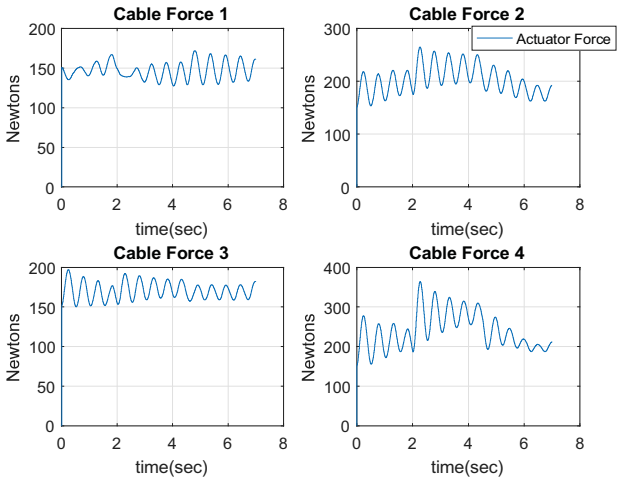

Fig. 8. simulated Cables forces.

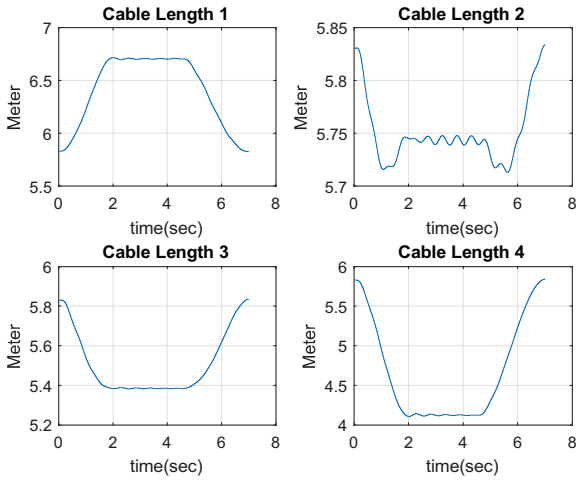

Fig. 9. Cables lengths in the simulation.

Automatic Control, IEEE Transactions on, vol. 46, no. 8, pp. 1313–1318, 2001.

[7] C. C. Cheah, M. Hirano, S. Kawamura, and S. Arimoto, "Approximate jacobian control for robots with uncertain kinematics and dynamics," *Robotics and Automation, IEEE Transactions on*, vol. 19, no. 4, pp. 692–702, 2003.

[8] C.-C. Cheah, C. Liu, and J.-J. E. Slotine, "Adaptive jacobian tracking control of robots with uncertainties in kinematic, dynamic and actuator models," *IEEE transactions on automatic control*, vol. 51, no. 6, pp. 1024–1029, 2006.

[9] C. C. Cheah and X. Li, *Task-space sensory feedback control of robot manipulators*. Springer, 2015, vol. 73.

[10] G. Bartolini, A. Ferrara, A. Levant, and E. Usai, "On second order sliding mode controllers," in *Variable structure systems, sliding mode and nonlinear control*. Springer, 1999, pp. 329–350.

[11] G. Bartolini, A. Pisano, E. Punta, and E. Usai, "A survey of applications of second-order sliding mode control to mechanical systems," *International Journal of control*, vol. 76, no. 9-10, pp. 875–892, 2003.

[12] H. Sira-Ramírez, "On the sliding mode control of nonlinear systems," *Systems & control letters*, vol. 19, no. 4, pp. 303–312, 1992.

[13] G. Bartolini, A. Levant, A. Pisano, and E. Usai, "Adaptive second-order sliding mode control with uncertainty compensation," *International Journal of Control*, vol. 89, no. 9, pp. 1747–1758, 2016.

[14] R. Babaghasabha, M. A. Khosravi, and H. D. Taghirad, "Adaptive robust control of fully-constrained cable driven parallel robots," *Mechatronics*, vol. 25, pp. 27–36, 2015.

[15] M. A. Arteaga, A. Castillo-Sánchez, and V. Parra-Vega, "Cartesian control of robots without dynamic model and observer design," *Automatica*, vol. 42, no. 3, pp. 473–480, 2006.

[16] V. Parra-Vega, S. Arimoto, Y.-H. Liu, G. Hirzinger, and P. Akella, "Dynamic sliding pid control for tracking of robot manipulators: Theory and experiments," *IEEE Transactions on Robotics and Automation*, vol. 19, no. 6, pp. 967–976, 2003.

[17] R. Garcia-Rodriguez and V. Parra-Vega, "Cartesian sliding pid control schemes for tracking robots with uncertain jacobian," *Transactions of the Institute of Measurement and Control*, vol. 34, no. 4, pp. 448–462, 2012.

[18] A. J. Koshkouei, K. J. Burnham, and A. S. Zinober, "Dynamic sliding mode control design," *IEE Proceedings-Control Theory and Applications*, vol. 152, no. 4, pp. 392–396, 2005.

[19] M.-S. Chen, C.-H. Chen, and F.-Y. Yang, "An ltr-observer-based dynamic sliding mode control for chattering reduction," *Automatica*, vol. 43, no. 6, pp. 1111–1116, 2007.

[20] H. Taghirad, *Parallel robots: mechanics and control*. taylor & francis, 2012.